

Article scientifique

Article

2024

Published version

Open Access

This is the published version of the publication, made available in accordance with the publisher's policy.

---

## Population Pharmacokinetics of Cabotegravir Following Oral Administration and Long-Acting Intramuscular Injection in Real-World People with HIV

---

Thoueille, Paul; Saldanha, Susana Alves; Schaller, Fabian; Choong, Eva; Veuve, François; Munting, Aline; Cavassini, Matthias; Braun, Dominique; Günthard, Huldrych F.; Duran Ramirez, Jessy J.; Surial, Bernard; Furrer, Hansjakob; Rauch, Andri; Ustero Alonso, Pilar **[and 10 more]**

Collaborators: Kaiser, Laurent; Keiser, Olivia; Martinez De Tejada Weber, Begona; Yerly Ferrillo, Sabine

### How to cite

THOUEILLE, Paul et al. Population Pharmacokinetics of Cabotegravir Following Oral Administration and Long-Acting Intramuscular Injection in Real-World People with HIV. In: *Clinical pharmacology and therapeutics*, 2024, vol. 115, n° 6, p. 1450–1459. doi: 10.1002/cpt.3240

This publication URL: <https://archive-ouverte.unige.ch/unige:180688>

Publication DOI: [10.1002/cpt.3240](https://doi.org/10.1002/cpt.3240)

# Population Pharmacokinetics of Cabotegravir Following Oral Administration and Long-Acting Intramuscular Injection in Real-World People with HIV

Paul Thoueille<sup>1,2</sup> , Susana Alves Saldanha<sup>1</sup>, Fabian Schaller<sup>1</sup>, Eva Choong<sup>1</sup> , François Veuve<sup>1</sup>, Aline Munting<sup>3</sup> , Matthias Cavassini<sup>3</sup> , Dominique Braun<sup>4,5</sup> , Huldrych F. Günthard<sup>4,5</sup> , Jessy J. Duran Ramirez<sup>4,5</sup> , Bernard Surial<sup>6</sup> , Hansjakob Furrer<sup>6</sup> , Andri Rauch<sup>6</sup> , Pilar Ustero<sup>7</sup> , Alexandra Calmy<sup>7,8</sup> , Marcel Stöckle<sup>9</sup>, Caroline Di Benedetto<sup>10</sup>, Enos Bernasconi<sup>11</sup> , Patrick Schmid<sup>12</sup>, Catia Marzolini<sup>1,9,13</sup> , François R. Girardin<sup>1,2</sup> , Thierry Buclin<sup>2</sup> , Laurent A. Decosterd<sup>1</sup> , Monia Guidi<sup>2,14,15,\*</sup>  and the Swiss HIV Cohort Study

Long-acting cabotegravir has been studied mainly in the stringent framework of clinical trials, which does not necessarily reflect the situation of people with HIV (PWH) in routine clinical settings. The present population pharmacokinetic analysis aims to build real-world reference percentile curves of cabotegravir concentrations, accounting for patient-related factors that may affect cabotegravir exposure. The second objective is to simulate whether dosing interval adjustments of cabotegravir could be considered in specific subpopulations. Overall, 238 PWH contributed to 1,038 cabotegravir levels (186 during the initial oral administration phase and 852 after intramuscular injection). Cabotegravir pharmacokinetics was best described using a one-compartment model with distinct first order-absorption for oral and intramuscular administrations, and identical volume and clearance. Our model showed almost 40% faster absorption and 30% higher clearance than previously reported, resulting in a time to steady-state of 8 months and an elimination half-life of 4.6 weeks for long-acting cabotegravir. Sex and body mass index significantly influenced absorption, and bodyweight affected clearance. Model-based simulations showed that cabotegravir trough concentrations in females were 25% lower 4 weeks after the intramuscular loading dose, but 42% higher during the late maintenance phase. Finally, simulations indicated that in females, despite significantly higher cabotegravir concentrations, longer intervals between injections may not consistently ensure levels above the 4-fold protein-adjusted 90% inhibitory target concentration.

## Study Highlights

### WHAT IS THE CURRENT KNOWLEDGE ON THE TOPIC?

Available population pharmacokinetic (PopPK) models of cabotegravir concentrations after intramuscular injection are based on phase IIa/III studies.

### WHAT QUESTION DID THIS STUDY ADDRESS?

Despite exhibiting significant pharmacokinetic (PK) variability of the same order of magnitude as previously reported in registration studies, cabotegravir concentrations observed in our real-world nationwide observational study were substantially lower than previously reported.

### WHAT DOES THIS STUDY ADD TO OUR KNOWLEDGE?

Our PopPK model shows a faster absorption rate constant and elimination than previously described, resulting in lower

trough concentrations of cabotegravir. Sex was found to have a strong effect on the long-acting cabotegravir absorption rate.

### HOW MIGHT THIS CHANGE CLINICAL PHARMACOLOGY OR TRANSLATIONAL SCIENCE?

This analysis highlights discrepancies in PK between clinical trial participants and people with HIV followed in a routine clinical setting, and provides the basis for further studies on their implications for clinical care. In addition, simulations show that 3-monthly injections of cabotegravir might not consistently provide exposure levels ensuring effectiveness.

Received December 18, 2023; accepted February 25, 2024. doi:10.1002/cpt.3240

<sup>1</sup>Laboratory of Clinical Pharmacology, Department of Laboratory Medicine and Pathology, Lausanne University Hospital and University of Lausanne, Lausanne, Switzerland; <sup>2</sup>Service of Clinical Pharmacology, Department of Medicine, Lausanne University Hospital and University of Lausanne, Lausanne, Switzerland; <sup>3</sup>Service of Infectious Diseases, Department of Medicine, Lausanne University Hospital and University of Lausanne, Lausanne, Switzerland; <sup>4</sup>Department of Infectious Diseases and Hospital Epidemiology, University Hospital Zurich, Zurich, Switzerland; <sup>5</sup>Institute of Medical Virology, University of Zurich, Zurich, Switzerland; <sup>6</sup>Department of Infectious Diseases, Inselspital, Bern University Hospital, University of Bern, Bern, Switzerland; <sup>7</sup>Division of Infectious Diseases, Faculty of Medicine, Geneva University Hospitals, Geneva, Switzerland; <sup>8</sup>Department of Medicine, Faculty of Medicine, University of Geneva, Geneva, Switzerland; <sup>9</sup>Division of Infectious Diseases and Hospital Epidemiology, University Hospital Basel, University of Basel, Basel, Switzerland; <sup>10</sup>Division of Infectious Diseases, Ente Ospedaliero Cantonale, Lugano, Switzerland; <sup>11</sup>Division of Infectious Diseases, Ente Ospedaliero Cantonale, Lugano, University of Geneva, and University of Southern Switzerland, Lugano, Switzerland; <sup>12</sup>Division of Infectious Diseases and Hospital Epidemiology, Cantonal Hospital St. Gallen, St. Gallen, Switzerland; <sup>13</sup>Department of Molecular and Clinical Pharmacology, Institute of Translational Medicine, University of Liverpool, Liverpool, UK; <sup>14</sup>Centre for Research and Innovation in Clinical Pharmaceutical Sciences, Lausanne University Hospital and University of Lausanne, Lausanne, Switzerland; <sup>15</sup>Institute of Pharmaceutical Sciences of Western Switzerland, University of Geneva, University of Lausanne, Geneva, Switzerland. \*Correspondence: Monia Guidi ([monia.guidi@chuv.ch](mailto:monia.guidi@chuv.ch))

The Swiss HIV Cohort Study members are present in the Acknowledgment section.

Cabotegravir is an integrase strand transfer inhibitor with a high antiviral potency.<sup>1</sup> It is formulated as a once-daily oral tablet and a nanosuspension to be injected intramuscularly (i.m.). The nanosuspension technology increases the apparent half-life of elimination ( $t_{1/2}$ ) of cabotegravir from 41 hours to approximately 5.6–11.5 weeks.<sup>2–4</sup> Cabotegravir in combination with rilpivirine is the first long-acting complete regimen for the maintenance treatment of HIV-1 infection in adults.<sup>2,3,5</sup> After an optional one-month oral lead-in period, a loading dose of 600/900 mg of cabotegravir/rilpivirine is injected i.m., followed 4 weeks later by the i.m. maintenance dose of 600/900 mg of cabotegravir/rilpivirine every 2 months, or the i.m. maintenance dose of 400/600 mg of cabotegravir/rilpivirine every month in some regions. In addition to its use for HIV infection treatment, long-acting i.m. cabotegravir was found to be superior to the oral tenofovir disoproxil fumarate/emtricitabine combination and was approved by the US Food and Drug Administration (FDA) for pre-exposure prophylaxis (PrEP) in at-risk adults and adolescents to prevent the risk of HIV acquisition.<sup>6–8</sup> In the absence of an effective vaccine, such i.m. chemoprevention overcomes adherence issues with oral PrEP by ensuring month-long effective plasma concentrations and is likely to play an increasing role among effective HIV prevention options, particularly in high-incidence regions where resources are limited and needs are greatest.

Population pharmacokinetic (PopPK) analyses of long-acting cabotegravir based on data from phase IIa/III trials – which included healthy volunteers, HIV-uninfected and at low-risk for HIV, and carefully selected HIV-1 infected individuals – allowed characterizing drug concentration-time profiles by a two-compartment model with first-order absorption and linear elimination, associated with extensive pharmacokinetic (PK) variability.<sup>9,10</sup> Body mass index (BMI) and sex were shown to affect significantly cabotegravir PKs. In particular, the absorption rate constant of i.m. cabotegravir was found to be more than 40% slower in females compared with males.<sup>9,10</sup> Considering the inherent “flip-flop” kinetics of long-acting cabotegravir, a slower absorption rate would lead to lower peak concentrations, but elevated trough concentrations ( $C_{trough}$ ). Therefore, females are expected to have higher  $C_{trough}$  of cabotegravir than males and may be at lower risk for subtherapeutic exposure. The protein-adjusted cabotegravir concentration required for 90% inhibition of viral replication (PAIC<sub>90</sub>) is 166 ng/mL.<sup>11</sup> However, higher clinical target thresholds, that is, 4xPAIC<sub>90</sub>, are recommended based on available drug exposure-response studies.<sup>12</sup>

In particular, the 4xPAIC<sub>90</sub> threshold was reported to be associated with high protective efficacy in rectal and vaginal simian HIV challenge models.<sup>12</sup> This target also corresponds to the fifth percentile of cabotegravir  $C_{trough}$  observed after the loading injection in phase III and PrEP trials.<sup>13,14</sup>

The present PopPK analysis is part of a nationwide multicenter observational study within the Swiss HIV Cohort Study (SHCS) for the prospective monitoring of people with HIV (PWH) on long-acting cabotegravir/rilpivirine.<sup>15</sup> This analysis constitutes the first characterization of the concentration-time profile of long-acting cabotegravir and its associated variability among PWH in a routine clinical setting. Because PWH on long-acting cabotegravir/rilpivirine are mostly monitored by viral load measurements and in a few settings also by therapeutic drug monitoring (TDM), the main objective is to build real-world reference percentile curves of cabotegravir concentrations that can be used to support the interpretation of TDM results in PWH receiving this treatment.<sup>16</sup> For clarity, the reference curves of rilpivirine are described in a separate paper. The second objective of the study is to ascertain whether it would be possible to extend the time interval between injections of cabotegravir in specific subpopulations, using model-based Monte Carlo simulations.

## METHODS

### Study population

The SHCS is a prospective longitudinal study for the follow-up of PWH in Switzerland. The SHCS was established in 1988 and represents ~72% of all people on antiretroviral therapy in Switzerland.<sup>17</sup> Written informed consent was obtained from all participants and the SHCS was approved by ethics committees. Following the approval of long-acting cabotegravir/rilpivirine in Switzerland in March 2022, drug samples were collected longitudinally at the discretion of physicians until June 2023. Adults (>18 years old) receiving long-acting cabotegravir/rilpivirine enrolled in the nationwide observational study were included in this PopPK analysis.<sup>15</sup> Blood sampling and last administration times, dosage, individual body weight (BW), height, and BMI were recorded. Relevant clinical and demographic information, namely age, sex at birth, CD4 cell count, ethnicity, viral load, and co-medications were extracted from the SHCS database. Exclusion criteria were undetectable plasma concentration after oral administration (suggesting nonadherence to oral treatment), and non-reliable information on time and/or date of last drug administration and/or blood collection. Finally, a detailed PK substudy was proposed to consenting PWH followed up in Lausanne or Geneva, and implied blood sampling just before cabotegravir/rilpivirine injection, and at 1, 2, 4, and 8 weeks ( $C_{trough}$ ) postdose (Project-ID 2022–00619, approved by the Canton's Ethics Committee, Lausanne, Switzerland).

## Analytical method

Samples were analyzed by multiplex high-performance liquid chromatography coupled to tandem mass spectrometry, using a previously published validated method.<sup>18</sup> The lower limit of quantification (LLOQ) was 25 ng/mL.

## Population pharmacokinetic analysis

The nonlinear mixed effects modeling software (NONMEM version 7.5.1, ICON Development Solutions, Ellicott City, MD) was used with PsN (version 5.3.1) and Pirana (version 2.9.3). Data management, graphical exploration, and statistical analyses were performed with R (version 4.1.1, R Development Core Team, <http://www.r-project.org/>). Steady-state was assumed for all samples collected during the oral lead-in period, as samples were collected at least 2 weeks after treatment initiation, just prior to the injection of the i.m. loading dose.<sup>19</sup> Regarding i.m. injections, steady-state was assumed 44 weeks after the loading dose, in accordance with previous studies.<sup>20,21</sup> Observations below the LLOQ were handled by setting the values at LLOQ/2.<sup>22</sup>

## Base and covariate models

A stepwise procedure was used to identify the best model for cabotegravir concentrations after oral and i.m. administrations, comparing various compartmental dispositions with linear elimination and absorption processes. Differential equations (ADVAN13) were used to specify the models in NONMEM to best depict the dynamics of the longitudinal data collected. Because of the small number of samples collected immediately after oral drug intake, the first-order absorption rate ( $k_{a-oral}$ ) was fixed to 1.12 h<sup>-1</sup> based on preliminary model development, in accordance with the published value.<sup>9</sup> Parametrization was done in terms of apparent clearance ( $CL$ ) and volume of distribution ( $V$ ), in addition to the respective absorption rate constants (i.e.,  $k_{a-oral}$  and  $k_{a-LA}$  for oral and i.m. absorption, respectively). All parameters were assumed to follow a log-normal distribution, and between-subject variability (BSV) was sequentially tested for all of them. Interoccasion variability (IOV) was considered for i.m. administration only, to account for within-subject variability between injections (e.g., injection-related variability and unexplained physiological differences). Specifically, an “occasion” variable was built with an incremental number within each subject for a maximum of six occasions, consistent with the duration of the follow-up period in the long-acting phase. Lastly, distinct residual unexplained variabilities (RUVs) were evaluated for oral and i.m. administrations.

The following covariates were tested for significance on the base model parameters, using linear or allometric functions as deemed appropriate: age, sex at birth, ethnicity, BW, BMI, height, eGFR categories classified according to the Chronic Kidney Disease Epidemiology Collaboration (CKD-EPI) equations,<sup>23</sup> and liver cirrhosis classified according to the Child-Pugh score.<sup>24</sup> Ethnicity was first modeled by assigning a separate  $CL$  per group and then per regrouped ethnicities. Concomitant drugs, such as UGT1A1 inducers, considered clinically relevant,<sup>8,25</sup> were not encountered in the included PWH.

## Model selection and evaluation

Hierarchical models were statistically discriminated using the variation of the NONMEM objective function value ( $\Delta OFV$ ) at a significance level of 0.05 in forward model building ( $\Delta OFV < -3.84$  for one additional parameter), and of 0.01 in backward deletion ( $\Delta OFV > 6.63$  for the removal of one parameter) steps. Otherwise, Akaike's information criterion was used for non-hierarchical models. In addition to the statistical criterion, covariates were retained in the model according to clinical considerations and to the quantification of BSV explained by their introduction. The accuracy of PK parameter estimates, quantified by the relative standard error, and goodness-of-fit diagnostic and individual plots helped in model selection. The characterization

of model shrinkage (i.e.,  $\varepsilon$ -shrinkage and  $\eta$ -shrinkage referring to the RUV and BSV, respectively) also helped to assess the reliability of the results.

Prediction- and variability-corrected visual predictive checks (pvcVPCs) were performed on the final PopPK model, including covariates to compare the observed concentrations with the 5th, 50th, and 95th prediction percentiles.<sup>26-28</sup> The bootstrap method ( $n = 2000$ )<sup>26</sup> contributed to the model reliability assessment by comparing the original model estimates to the bootstrap median parameter values and their 95% confidence intervals. Finally, cross-validation was performed through repeated data-splitting ( $n = 5$ ) to generate random subsets of the dataset (80% in the learning and 20% in the validation subset). Log-transformed observed and individual predicted concentrations of the validation dataset were compared with mean prediction error (MPE) and root mean square error to quantify the model accuracy and precision, respectively.<sup>29</sup>

## Model-based Monte Carlo simulations

Model-based simulations were performed to generate population percentiles for cabotegravir after oral and i.m. administrations at predefined levels of the retained covariates, by simulating 1,000 individuals in each group to infer the corresponding cabotegravir  $C_{trough}$ . For continuous covariates, a normal distribution within clinically relevant ranges was assumed to generate individual values; for instance, we generated 1,000 virtual individuals across three BMI categories (i.e.,  $BMI < 25 \text{ kg/m}^2$ ,  $BMI 25-30 \text{ kg/m}^2$ , and  $BMI > 30 \text{ kg/m}^2$ ), assuming a normal distribution within each BMI category, while also maintaining correlated BW within each category, under the assumption of a normal distribution as well. On the other hand, the effects of categorical covariates were evaluated by comparing 1,000 PK profiles simulated in each category. Model-based simulations helped to assess the clinical relevance of the selected covariates, explore the impact of delayed injections, and provided a rational basis for potential dosage adjustment.

## RESULTS

Overall, 238 PWH contributed 1,038 cabotegravir levels (186 after oral administration and 852 after i.m. injection). A total of 28 PWH underwent detailed PK sampling. The unique concentration detected below the quantification limit (~1 ng/mL) was collected more than 6 months after treatment discontinuation. The median follow-up duration was 26 weeks (range: 3–196), with a median time between injections of 56 (0–186) days, and a median of 4 (1–15) samples collected per individual. **Table 1** summarizes the characteristics of the study population.

## Structural, statistical, and covariate models

A one-compartment model with distinct first order-absorption for oral and i.m. administrations (i.e.,  $k_{a-oral}$  and  $k_{a-LA}$ ), and identical  $CL$  and  $V$  depicting cabotegravir linear disposition best described the data (**Figure 1**). When administered i.m., cabotegravir exhibited “flip-flop” kinetics (i.e., absorption rate constant  $k_{a-LA} <$  elimination rate constant  $k_e = CL/V$ ) consistent with published models.<sup>9,10</sup> BSV was retained on  $k_{a-LA}$  and  $V$  ( $\Delta OFV = -122$  and  $-14$ ,  $P < 0.001$ , respectively). Models incorporating an oral to i.m. relative bioavailability were investigated. However, similar bioavailabilities were calculated, suggesting a similar disposition between oral and i.m. cabotegravir, and therefore this parameter was not retained. On another note, IOV was supported for  $CL$  after i.m. administration ( $\Delta OFV = -68$ ,  $P < 0.001$ ). A proportional error model best described cabotegravir RUV after oral administration,

**Table 1** Characteristics of the study population

Population characteristics	
Last recorded value	Median (range) or n (%)
Sex	
Male	190 (80)
Female	48 (20)
Age, years	46 (20–79)
Ethnicity	
White	133 (56)
Black	36 (15)
Hispanic American	19 (8)
Asian	11 (5)
Other/missing	39 (16)
Body weight, kg	78 (50–126)
Height, cm	176 (151–198)
BMI, kg/m <sup>2</sup>	25.4 (18.2–43.3)
<25	104 (44)
25–30	103 (43)
>30	31 (13)
eGFR <sup>a</sup> , mL/min/1.73 m <sup>2</sup> <sup>23</sup>	
G1: ≥90	158 (66)
G2: 60–89	76 (32)
G3: 30–59	4 (2)
Liver cirrhosis <sup>a</sup> , Child-Pugh score <sup>24</sup>	
No	236 (99)
Class A	2 (1)
CD4 cell count, cells/mm <sup>3</sup>	
≥500	186 (78)
350 to <500	23 (10)
<350	29 (12)
Plasma HIV RNA, copies/mL	
<50	233 (98)
≥50 and <200	4 (2)
≥200	1 (<1)

BMI, body mass index; eGFR, estimated glomerular filtration rate, calculated according to the Chronic Kidney Disease Epidemiology Collaboration (CKD-EPI) equations reported by Levey *et al.*<sup>23</sup>

<sup>a</sup>≤2% missing information.

whereas a mixed error model was retained for cabotegravir RUV when administered i.m. Parameter estimates of the base PopPK model with BSV (coefficient of variation %) were:  $k_{a-oral}$  of 1.12 h<sup>-1</sup> (fixed),  $k_{a-LA}$  of 0.000888 h<sup>-1</sup> (47.1%),  $V$  of 7.57 L (103.5%), and  $CL$  of 0.203 L/h (27.4% with an IOV of 27.4%).

Univariate analyses revealed clear effects of female sex ( $\Delta OFV = -28$ ,  $P < 0.001$ ), height ( $\Delta OFV = -18$ ,  $P < 0.001$ ), and BMI ( $\Delta OFV = -16$ ,  $P < 0.001$ ) on  $k_{a-LA}$ . In addition, BW ( $\Delta OFV = -13$ ,  $P < 0.001$ ) and BMI ( $\Delta OFV = -6$ ,  $P < 0.05$ ) significantly affected cabotegravir  $CL$ . After backward deletion, the final model included linear effects of female sex and BMI on  $k_{a-LA}$ , whereas BW affected  $CL$  through an allometric scaling relation:

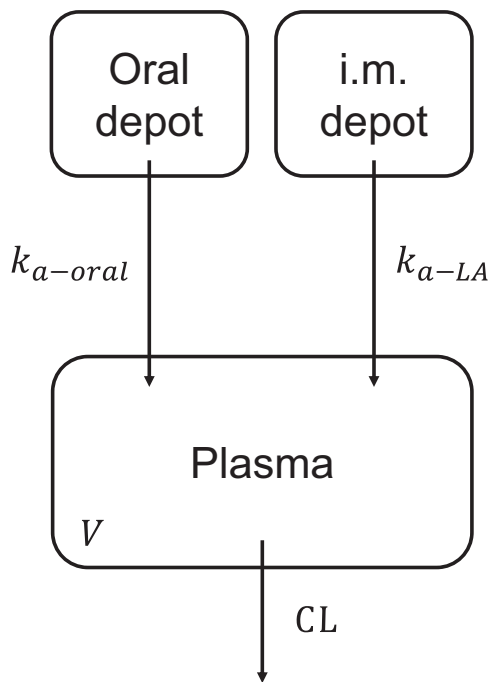


**Figure 1** Structural model used to describe cabotegravir concentration-time profiles. CL, apparent clearance; i.m., intramuscular;  $k_{a-LA}$ , first-order absorption rate constant for long-acting administration;  $k_{a-oral}$ , first-order absorption rate constant for oral administration;  $V$ , apparent volume of distribution.

$$k_{a-LA_i} = k_{a-LA} \times (1 + \theta_{Female}) \times \left( 1 + \theta_{BMI} \times \frac{(BMI - BMI_M)}{BMI_M} \right) \times e^{\eta_{i,k_{a-LA}}}$$

$$CL_i = CL \times \left( \frac{BW}{BW_M} \right)^{\theta_{BW}} \times e^{\eta_{i,CL}} \times e^{\kappa_{ij}}$$

Where the  $\theta$  denote the estimated parameters for covariate effects,  $BMI_M$  and  $BW_M$  are the median values in the study population,  $k_{a-LA}$  and  $CL$  are the typical values in our population,  $k_{a-LA_i}$  and  $CL_i$  are the individual values for the  $i$ th subject, and the  $\eta_i$  and  $\kappa_{ij}$  are the BSV and IOV terms, respectively.

The results showed that females had a  $k_{a-LA}$  40.5% slower than males. Similarly, individuals with a BMI of 35 kg/m<sup>2</sup> would have a  $k_{a-LA}$  of 0.00062 h<sup>-1</sup>, 39% lower than the  $k_{a-LA}$  of 0.00102 h<sup>-1</sup> obtained in those with a median BMI (i.e., 25.2 kg/m<sup>2</sup>). On the other hand, people with a BW of 100 kg would have a  $CL$  of 0.225 L/h, only 12% higher than those with a median BW (i.e., 78 kg) having a  $CL$  of 0.201 L/h. Finally, the covariates included in the final PopPK model explained 34% of the BSV on  $k_{a-LA}$ , with 27% resulting from the inclusion of sex alone, and 12% of the BSV on  $CL$ .

### Model evaluation

**Figure S1** shows the goodness-of-fit diagnostic plots of the final model, whereas **Figure S2** compares the BSV distribution for each retained covariates before and after covariates inclusion. Of note, there was a modest shrinkage of 37% on  $k_{a-LA}$  BSV, rendering the

use of classic diagnostic plots of diminished value.<sup>30</sup> Nevertheless, the pvcVPC and the bootstrap results, shown in **Figure 2** and **Table 2**, respectively, confirm the reliability of the final model. Finally, cross-validation (**Table S1**) did not reveal any significant bias (mean MPE = 2.1%, mean 95% confidence interval = -1.3% to 5.6%) with a precision of 27.1% (range: 23.1–33.1%).

### Model-based Monte Carlo simulations

Model-based simulations showed a median cabotegravir  $C_{\text{trough}}$  of 4,410 ng/mL (95% prediction interval (PI<sub>95</sub>): 454–8,392 ng/mL) at steady-state after oral administration (**Figure S3**). Regarding long-acting cabotegravir, the median  $C_{\text{trough}}$  was 25% lower in females 4 weeks after the loading dose, compared with males, amounting to 1,231 (PI<sub>95</sub>: 501–3,102) ng/mL vs. 1,645 (PI<sub>95</sub>: 669–3,830) ng/mL, respectively (**Figure 3**, **Table S2**). However, the difference in  $C_{\text{trough}}$  between the two groups inverted during the late maintenance phase, reaching trough levels 42% higher in females at week 48, with a median  $C_{\text{trough}}$  of 1,486 (PI<sub>95</sub>: 632–3,326) ng/mL predicted in females vs. 1,043 (PI<sub>95</sub>: 367–2,544) ng/mL in males. In addition, simulations accounting for the effect of BMI range (i.e., BMI < 25 kg/m<sup>2</sup>, BMI 25–30 kg/m<sup>2</sup>, and BMI > 30 kg/m<sup>2</sup>) with correlated BW (**Figure S4**, 1,000 individuals in each group) showed that overall, obese individuals (i.e., BMI > 30 kg/m<sup>2</sup>) had slower  $k_{a-LA}$  and therefore lower concentrations at week 8 (i.e., 4 weeks after the loading dose). In particular, obese females are predicted to have the lowest  $C_{\text{trough}}$  at week 8, with < 75% reaching the 4xPAIC<sub>90</sub> threshold. However, higher BMI (and correlated BW) leads to higher  $C_{\text{trough}}$  in the medium-term (i.e., from week 16 onward). Thus, males with a normal weight (i.e., BMI < 25 kg/m<sup>2</sup>)

were more susceptible to exhibit low exposure, with only 80% maintaining  $C_{\text{trough}}$  above the 4xPAIC<sub>90</sub> threshold from week 16 to week 48. In addition, **Table S3** shows the impact of delayed injections on  $C_{\text{trough}}$  in females and males over 48 weeks of follow-up. Consistent with our previous observations, females appear to be less susceptible to low  $C_{\text{trough}}$  with delayed injections, with more than 90%, 85%, and 80% remaining above the 4xPAIC<sub>90</sub> threshold when injections are delayed by 1, 2, and 3 weeks, respectively.

Finally, **Figure 4** presents the simulated PK profiles of long-acting cabotegravir injected every 3 months instead of 2. These simulations show that only 65% of females are predicted to have  $C_{\text{trough}}$  above the 4xPAIC<sub>90</sub> threshold with a 3-monthly administration. In contrast, only 25% of males are predicted to have concentrations above this target. Moreover, nearly 10% of males would have  $C_{\text{trough}}$  just at PAIC<sub>90</sub> (i.e., 166 ng/mL) from weeks 20 to 44. The same conclusions can be drawn when BMI (and correlated BW) is taken into account in the analysis (**Figure S5**), but with significantly higher percentages below the thresholds, as discussed above for normal weight or overweight males (i.e., BMI < 25 kg/m<sup>2</sup> and BMI 25–30 kg/m<sup>2</sup>, respectively).

### DISCUSSION

The present study describes the first PopPK model of oral and long-acting i.m. cabotegravir in PWH in a routine clinical setting, while highlighting the effects of sex, BMI, and BW on cabotegravir exposure. Our PopPK model is fairly consistent with previously reported models based on phase IIa/III studies.<sup>9,10</sup> A previously described peripheral compartment could not be observed in our study, presumably because of insufficient data during the “PK

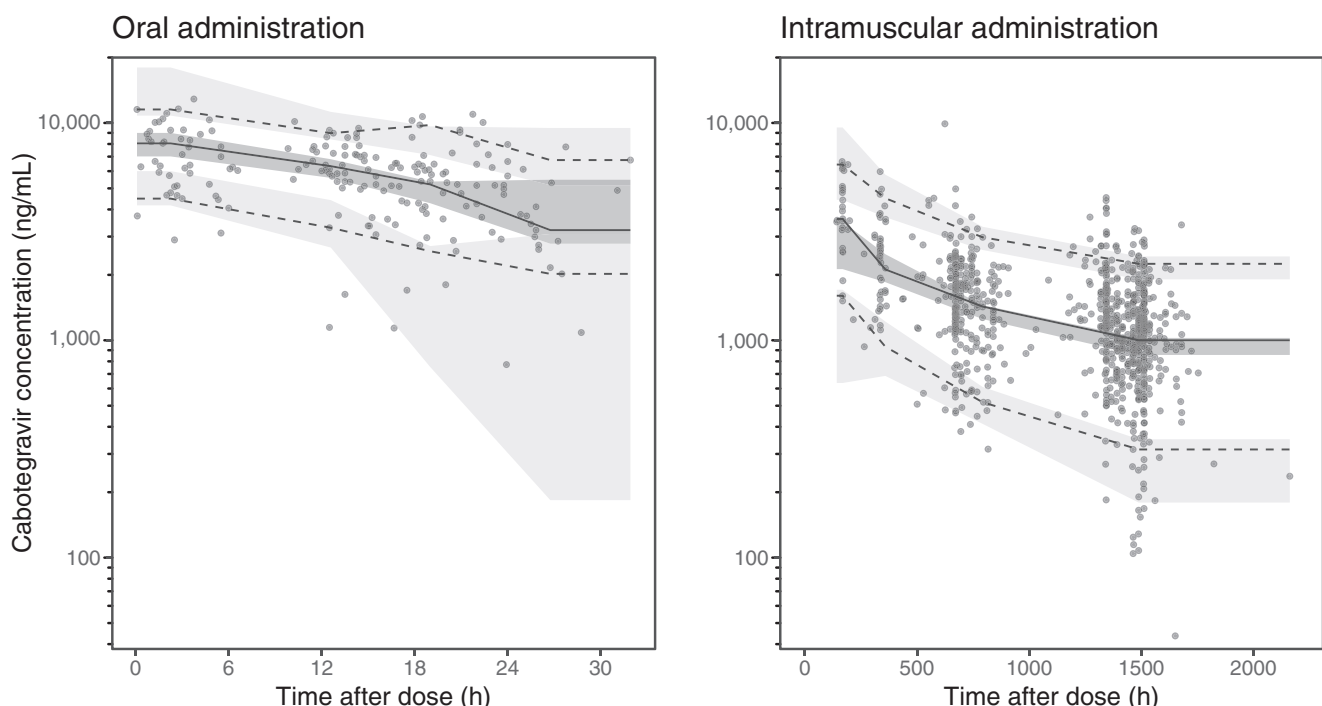


**Figure 2** Visual predictive check of the final cabotegravir PopPK model for oral administration (left panel) and intramuscular administration (right panel). Open circles represent the observed plasma concentrations. Solid and dashed lines represent the median and PI<sub>90%</sub> of the observed data, respectively. Shaded surfaces represent the model-predicted 90% confidence intervals of the simulated median and PI<sub>90%</sub>. One concentration with time beyond 4,000 hours is not displayed. PI<sub>90%</sub>, 90% prediction interval; PopPK, population pharmacokinetic.

**Table 2** Final population PK parameter estimates of cabotegravir with their bootstrap evaluations

Parameters	Final model	Bootstrap (n=2000)
	Estimate (RSE, %) <sup>b</sup>	Median [95% CI]
$k_{a\text{-oral}}$ (h <sup>-1</sup> )	1.12 FIX	1.12 FIX
$k_{a\text{-LA}}$ (h <sup>-1</sup> )	0.00102 (3)	0.00102 [0.000939–0.00111]
$\omega_{ka\text{-LA}}$ (CV% <sup>a</sup> )	37.7 (10)	36.9 [26.3–48.4]
$\theta_{\text{Female}}$	-0.405 (13)	-0.405 [-0.541 to -0.254]
$\theta_{\text{BMI}}$	-0.999 (20)	-0.999 [-1.410 to -0.455]
$V$ (L)	7.44 (12)	7.43 [6.04–9.29]
$\omega_V$ (CV%)	107.2 (14)	106.0 [75.7–129.0]
$CL$ (L/h)	0.201 (2)	0.200 [0.192–0.209]
$\omega_{CL}$ (CV% <sup>a</sup> )	25.6 (7)	25.2 [20.7–29.2]
$\omega_{IOV}$ (CV% <sup>a</sup> )	27.1 (8)	27.0 [21.6–31.8]
$\theta_{\text{Bodyweight}}$	0.460 (27)	0.460 [0.198–0.717]
$\sigma_{\text{prop-oral}}$ (CV% <sup>a</sup> )	11.4 (23)	11.4 [7.0–19.6]
$\sigma_{\text{prop-LA}}$ (CV% <sup>a</sup> )	20.4 (10)	20.4 [17.4–23.7]
$\sigma_{\text{add-LA}}$ (ng/mL)	194 (13)	192 [149–232]

Final model:

$$k_{a\text{-LA}_i} = k_{a\text{-LA}} \times (1 + \theta_{\text{Female}}) \times \left(1 + \theta_{\text{BMI}} \times \frac{(BMI - BMI_M)}{BMI_M}\right) \times e^{\eta_{ka\text{-LA}}}$$

$$CL_i = CL \times \left(\frac{BW}{BW_M}\right)^{\theta_{\text{BW}}} \times e^{\eta_{CL}} \times e^{\kappa_{ij}}$$

$k_{a\text{-oral}}$ : typical first-order absorption rate constant for oral administration;  $k_{a\text{-LA}}$ : typical first-order absorption rate constant for long-acting administration in our population;  $\theta_{\text{Female}}$ : effect of female sex on  $k_{a\text{-LA}}$ ;  $\theta_{\text{BMI}}$ : body mass index effect on  $k_{a\text{-LA}}$  and  $BMI_M = 25.2 \text{ kg/m}^2$ , median body mass index value in the study population;  $V$ : typical apparent volume of distribution in our population;  $CL$ : typical apparent clearance in our population;  $\theta_{\text{BW}}$ : bodyweight (BW) effect on  $CL$  and  $BW_M = 78 \text{ kg}$ , median bodyweight value in the study population;  $\omega_{IOV}$ : inter-occasion variability (IOV);  $\sigma_{\text{prop-oral}}$ : proportional residual error for oral administration;  $\sigma_{\text{prop-LA}}$ : proportional residual error for intramuscular administration;  $\sigma_{\text{add-LA}}$ : additive residual error for intramuscular administration.  $k_{a\text{-LA}_i}$ : individual value of  $k_{a\text{-LA}}$  in the  $i$ th subject;  $CL_i$ : individual value of  $CL$  in the  $i$ th subject;  $\eta_i$  and  $\kappa_{ij}$ : individual between-subject (BSV) and interoccasion (IOV) variability terms, independently estimated and normally distributed with mean zero and variances  $\omega^2$  and  $\omega_{IOV}^2$ , respectively.

<sup>a</sup>Coefficient of variation (CV, %) for BSV calculated as follows:  $\sqrt{(e^{\omega^2} - 1)}$ .

<sup>b</sup>Relative standard error (RSE) of the estimate, expressed as a percentage, with standard error (SE) of estimate, calculated as follows:

$$RSE (\%) = \frac{e^{\omega^2} \cdot SE}{2 \cdot (e^{\omega^2} - 1)}$$

tail." More importantly, our base model displays an almost 40% higher  $k_{a\text{-LA}}$  and an ~30% higher  $CL$ , compared with the parameter values reported by Han *et al.*<sup>9</sup> The "flip-flop" kinetics of the i.m. administration implies that the rate of absorption is the driving factor limiting drug disposition. Therefore, the faster absorption rate observed in our study hinders the desired prolonged effect to some extent, and the drug elimination process appears to occur earlier than previously estimated, together with a higher  $CL$ , thus resulting in lower  $C_{\text{trough}}$ . Our base model estimates an  $t_{1/2}$  of 4.6 weeks, shorter than literature values ranging from 5.6 to 11.5 weeks.<sup>2–4</sup> In addition, our data suggest that the steady-state is reached approximately 8 months after treatment initiation, also significantly faster than previously reported.<sup>3</sup> The reasons for

these discrepancies between clinical trial participants and PWH followed in a routine clinical setting remain unclear.

For oral cabotegravir, predicted  $C_{\text{trough}}$  was highly variable (i.e., PI<sub>95%</sub>: 454–8,392 ng/mL), likely amplified by imperfect adherence in some PWH resulting in lower predicted  $C_{\text{trough}}$ . Whereas our base model estimates a time to maximum concentration ( $T_{\text{max}}$ ) of 3.4 hours after oral administration, similar to previously reported values,<sup>3,19</sup> the  $t_{1/2}$  after oral administration was 26 hours, which is shorter than the mean value of 41 hours reported.<sup>3</sup>

Models incorporating an oral to i.m. relative bioavailability were investigated. Indeed, differences in cabotegravir bioavailability for different occasions would have been appropriate to plausibly reflect the biological variability affecting concentrations after i.m. injection. However, the bioavailabilities of the two routes of administration were not considered significantly different, and the model was thus not retained for subsequent analyses. Nonetheless, our PopPK model showed substantial BSV on PK parameters as well as significant IOV on  $CL$ . Preliminary analysis revealed an IOV on  $k_{a\text{-LA}}$  of 28.7%, which was in the same order of magnitude as the value reported by Yu *et al.*<sup>10</sup> However, this model was not stable enough to be implemented. In the absence of more informative data during the absorption phase, the IOV of  $k_{a\text{-LA}}$  could not be retained in the final model despite the differences in cabotegravir absorption and/or resorption appear to be a likely hypothesis to explain some of the IOV in cabotegravir exposure within subjects (e.g., injection-related variability,<sup>31</sup> as well as physiological differences). This lack of data probably also explains the modest shrinkage of 37% found on the BSV of  $k_{a\text{-LA}}$ .

The search for covariates revealed that sex had a highly significant effect on  $k_{a\text{-LA}_i}$  resulting in a lower  $C_{\text{trough}}$  predicted for females 4 weeks after the loading dose (i.e., at week 8), followed by significantly higher  $C_{\text{trough}}$  in females from weeks 16 to 48, consistent with previous analyses.<sup>9,10</sup> Males are indeed more likely to have low  $C_{\text{trough}}$  in the medium term, further modulated by the BMI. The BMI does not take into account fat distribution or muscle anatomy,<sup>32</sup> which arguably makes sex per se the relevant covariate driving differences in cabotegravir absorption. Noteworthy, it was found that the model with sex as the only covariate and the final model including sex, BMI, and BW performed similarly in predicting individual concentrations. Although the additional effects of BMI and BW are less clinically relevant, although highly statistically significant ( $P < 0.001$ ), than the influence of sex, they might represent additional risk factors for low exposure. Model-based simulations predict that obese individuals have initially lower  $C_{\text{trough}}$ . This is consistent with previously reported multi-variable analyses indicating that  $BMI > 30 \text{ kg/m}^2$  was associated with an increased risk of virologic failure (i.e., non-maintenance of undetectable viral load), in addition to HIV-1 subtype A6/A1, or cabotegravir and/or rilpivirine  $C_{\text{trough}}$  4 weeks after the initial loading dose.<sup>3,33,34</sup> According to our simulations and previous analyses, obese females would thus be at greater risk of insufficient exposure compared with other subpopulations because of cumulative risk factors. The decision to retain the three covariates in the final model was motivated by the existing evidence on risk factors for virologic failure and the availability of such covariates in routine clinical practice. It remains unclear at the moment whether

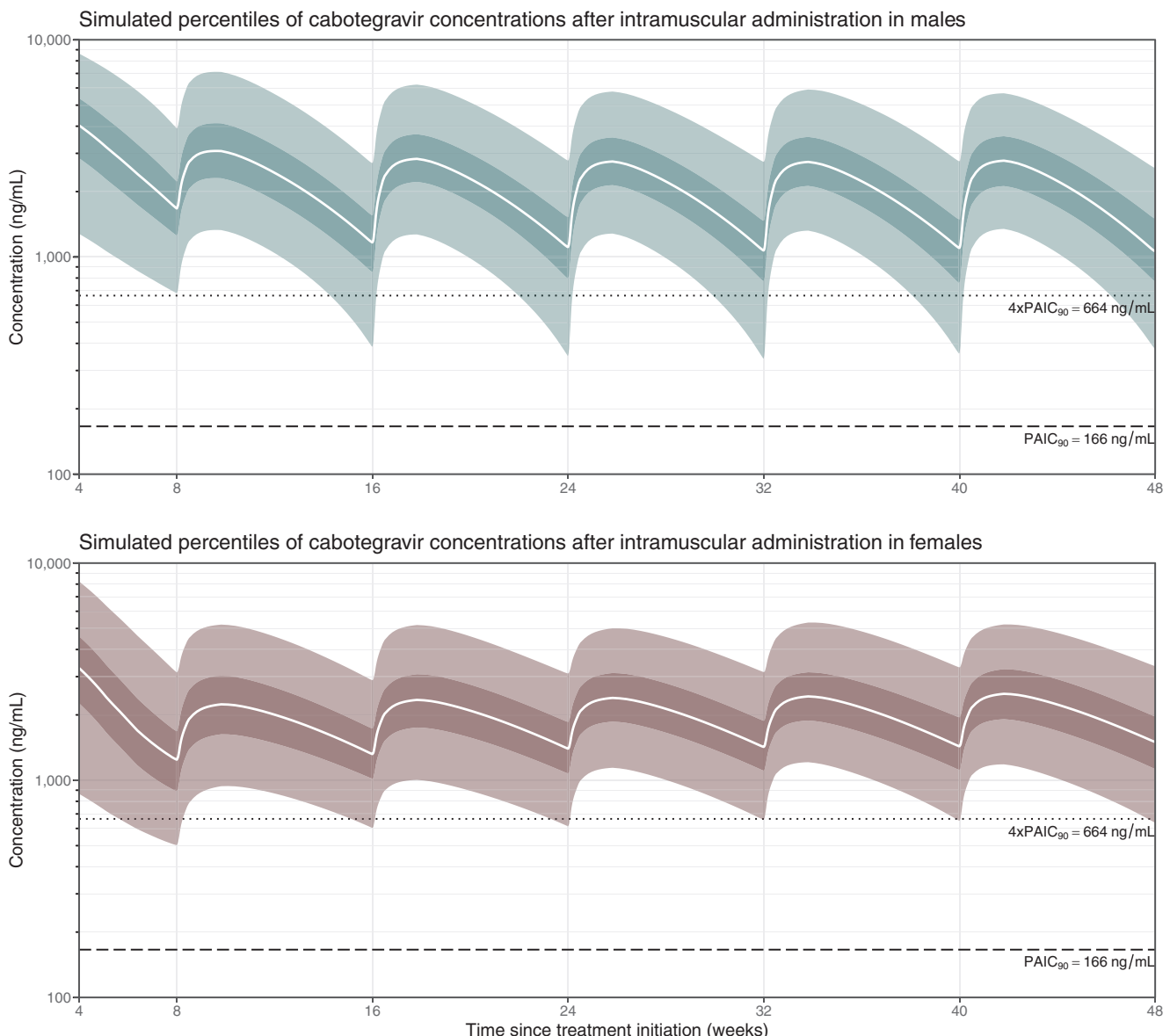


**Figure 3** Simulated percentiles, stratified by sex, after intramuscular administration of cabotegravir following a 4-week period of oral lead-in, using the model with sex only as a covariate. The solid white lines represent the median (50% percentile), whereas the dark surfaces encompass the 50% prediction intervals, and the light surfaces the 95% prediction intervals. PAIC, protein-adjusted inhibition concentration.

low plasma levels, associated with known, or as yet unrecognized risk factors, could compromise the therapeutic success of long-acting cabotegravir/rilpivirine.<sup>34</sup> Further prospective PK/pharmacodynamic studies are warranted.

The observational design offered limited occasions to capture early PK data on the first few days following injection. Yet, detailed PK sampling performed every week after injection revealed variable PK profiles among PWH, with a few individuals showing recurrently very low plasma concentrations already 1- or 2-week post injection. Whether such erratic PK profiles are due to either very slow resorption at injection site (i.e., the nanosuspension formulation sticks locally to tissues) or, conversely, to extremely rapid absorption and, in turn, elimination, cannot be addressed in our analysis. In our study, we did not have information on the needle length and injection technique, which could have affected the PK

of cabotegravir.<sup>9,35</sup> However, it is standard practice in Switzerland to use longer needles in obese patients, which limits the effect that this specific covariate may have had on cabotegravir PK. Limited data were obtained from morbidly obese PWH in our study. Importantly, a recent modeling study suggests that due to physiological changes (e.g., increased liver and renal blood flows with obesity), the patients who are morbidly obese PWH ( $BMI > 40 \text{ kg/m}^2$ ) are at higher risk of having suboptimal concentrations at the end of the dosing interval particularly for the bimonthly administration. TDM is advised in morbidly obese individuals as they may require monthly administrations of cabotegravir/rilpivirine,<sup>36</sup> and that obesity has been reported as one of the risk factors for virologic failure.<sup>34</sup> Finally, our PopPK model is based on real-world data obtained only in Switzerland, thus further studies are needed to ascertain whether our observations apply to other populations.

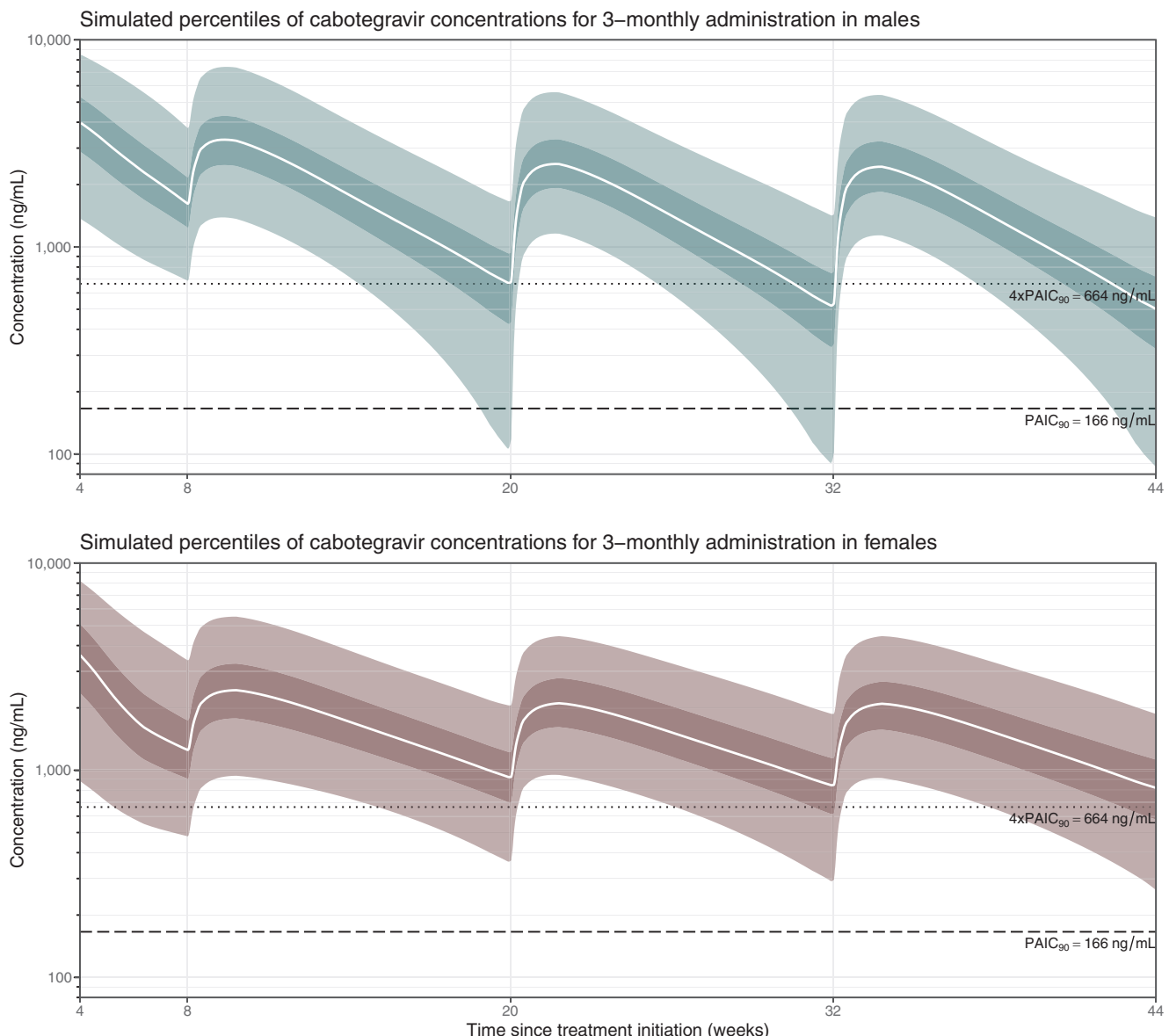


**Figure 4** Simulated cabotegravir concentration percentiles, stratified by sex, after 3-monthly intramuscular administration of cabotegravir following a 4-week period of oral lead-in, using the model with sex only as a covariate. The solid lines represent the median (50% percentile), whereas the surfaces encompass the 95% prediction intervals. PAIC, protein-adjusted inhibition concentration.

Combined sustained-release drug delivery technologies incorporating long-acting cabotegravir (or next generation long-acting antiretrovirals) with injectable contraceptives could help meet the urgent need for a wider range of effective HIV prevention options for women, particularly in high-incidence regions where resources are limited, and needs are greatest. Whether a trimestral injection of cabotegravir and contraceptives might be offered to female PW<sup>H</sup><sup>37</sup> still remains an open question. As previously reported, PK parameters are similar between HIV-negative participants and PW<sup>H</sup> in phase III trials.<sup>9,10</sup> Our model-based simulations show that 3-monthly injections of cabotegravir may not consistently provide levels anticipated to be highly protective in the context of PrEP (i.e., above 664 ng/mL).<sup>12,13</sup> In addition, given the significant IOV and BSV demonstrated by our PopPK model, punctual drops in cabotegravir  $C_{\text{trough}}$  may not be excluded. Further clinical studies

are thus necessary to understand the variables influencing IOV and to confidently personalize the dosing interval. In addition, some key issues remain unknown, such as the time to onset of protection with long-acting cabotegravir or the reasons for the emergence of HIV-1 infection despite on-time injections. Hazra *et al.*<sup>38</sup> recently reported the first case of HIV-1 infection despite *a priori* satisfactory cabotegravir concentrations at 7xPAIC<sub>90</sub>.

On another note, whereas the gluteal muscle is currently the only approved site for injection of long-acting antiretroviral, alternative body sites are being tested to expand antiretroviral delivery options.<sup>39</sup> For instance, no clinically relevant differences in cabotegravir (and rilpivirine) plasma concentrations were shown after gluteal or thigh administration.<sup>40</sup> However, absorption kinetics may differ between gluteal and alternative routes of administration, which may be influenced by differences in

muscle-fat tissue composition and other yet unidentified variables. Finally, new ultra-long-acting technologies are on the horizon with the potential to extend drug dosing intervals<sup>41,42</sup> by up to a year, thereby improving the convenience of the HIV prevention and treatment.

#### SUPPORTING INFORMATION

Supplementary information accompanies this paper on the *Clinical Pharmacology & Therapeutics* website ([www.cpt-journal.com](http://www.cpt-journal.com)).

#### ACKNOWLEDGMENTS

The authors would like to thank all people with HIV who participated in the study, as well as the physicians, nurses, data-collecting staff of the SHCS centers in Switzerland and the data and coordination center of the SHCS for excellent data management and administration. Open access funding provided by Université de Lausanne.

Members of the Swiss HIV Cohort Study: Abela I, Aebi-Popp K, Anagnostopoulos A, Battegay M, Bernasconi E, Braun DL, Bucher HC, Calmy A, Cavassini M, Ciuffi A, Dollenmaier G, Egger M, Elzi L, Fehr J, Fellay J, Furrer H, Fux CA, Günthard HF (President of the SHCS), Hachfeld A, Haerry D (deputy of "Positive Council"), Hasse B, Hirsch HH, Hoffmann M, Hösli I, Huber M, Jackson-Perry D (patient representatives), Kahlert CR (Chairman of the Mother & Child Substudy), Kaiser L, Keiser O, Klimkait T, Kouyos RD, Kovari H, Kusejko K (Head of Data Centre), Labhardt N, Leuzinger K, Martinez de Tejada B, Marzolini C, Metzner KJ, Müller N, Nemeth J, Nicca D, Notter J, Paioni P, Pantaleo G, Perreau M, Rauch A (Chairman of the Scientific Board), Salazar-Vizcaya L, Schmid P, Speck R, Stöckle M (Chairman of the Clinical and Laboratory Committee), Tarr P, Trkola A, Wandeler G, Weisser M, and Yerly S.

#### FUNDING INFORMATION

This independent work was funded by the Swiss National Science Foundation, grant number No 324730\_192449. This study was performed within the framework of the Swiss HIV Cohort Study, supported by the Swiss National Science Foundation (grant #201369), by SHCS project #879, and by the SHCS research foundation. The public funding source of the study had no role in the design of the study, in data collection, analysis and interpretation, in manuscript writing, or in the decision to submit the article for publication. This study received no support from pharmaceutical industries.

#### CONFLICT OF INTEREST STATEMENT

M.C. reports grants and payment for expert testimony from Gilead, MSD, and ViiV, and support for attending meetings from Gilead, paid to his institution. D.B. reports honoraria for advisory boards, lectures, and travel grants from the companies Gilead, ViiV, and MSD. H.F.G. has received unrestricted research grants from Gilead Sciences and ViiV Healthcare; fees for data and safety monitoring board membership from Merck; consulting/advisory board membership fees from Gilead Sciences, GSK, Johnson and Johnson, Janssen, Novartis, and ViiV Healthcare; and grants from the Yvonne Jacob Foundation, from National Institutes of Health, and unrestricted research grants from Gilead Sciences. The institution of J.J.D.R. received grants from Gilead Sciences and ViiV. B.S. reports support for travel grants and advisory boards from Gilead Sciences and ViiV, paid to his institution. The institution of H.F. received educational grants from ViiV, MSD, AbbVie, Gilead, and Sandoz. M.S. reports advisory board paid to his institution by Gilead, MSD, ViiV, Moderna, and Pfizer. The institution of A.R. received grants from Gilead; support for attending meetings from Gilead and Pfizer; and advisory boards from MSD and Moderna. C.M. has received speaker honoraria from ViiV, MSD, and Gilead. C.D.B. received travel grants for congress participation from Gilead. The institution of E.B. received grants from the Swiss National Science Foundation; grants from MSD; support for attending meetings from Gilead, MSD, ViiV, and Pfizer; and advisory boards from Gilead, MSD, ViiV, Pfizer, Moderna, AstraZeneca, AbbVie, and Lilly. The institution of P.S. received honoraria for advisory board and support for attending meetings from ViiV and Gilead. None of those grants and supports was related to the submitted work. All other authors declared no competing interests for this work.

#### AUTHOR CONTRIBUTIONS

P.T. wrote the manuscript. P.T., T.B., L.A.D., and M.G. designed the research. P.T., S.A.S., F.S., E.C., F.V., A.M., M.C., D.B., H.F.G., J.J.D.R., B.S., H.F., A.R., P.U., A.C., M.S., C.D.B., E.B., P.S., C.M., F.R.G., T.B., L.A.D., and M.G. performed the research. P.T. and M.G. analyzed the data.

#### DATA AVAILABILITY STATEMENT

A request for data sharing can be sent to the Scientific Board of the Swiss HIV Cohort Study (<https://www.shcs.ch>). A detailed explanation of the purpose for the request as well as a study protocol, if applicable, should be presented. The final decision about data release will be taken by the Scientific Board of the SHCS.

© 2024 The Authors. *Clinical Pharmacology & Therapeutics* published by Wiley Periodicals LLC on behalf of American Society for Clinical Pharmacology and Therapeutics.

This is an open access article under the terms of the [Creative Commons Attribution-NonCommercial License](https://creativecommons.org/licenses/by-nc/4.0/), which permits use, distribution and reproduction in any medium, provided the original work is properly cited and is not used for commercial purposes.

1. Trezza, C., Ford, S.L., Spreen, W., Pan, R. & Piscitelli, S. Formulation and pharmacology of long-acting cabotegravir. *Curr. Opin. HIV AIDS* **10**, 239–245 (2015).
2. U.S. Food and Drug Administration. Cabenuva product label <[https://www.accessdata.fda.gov/drugsatfda\\_docs/label/2022/212888s005s006lbl.pdf](https://www.accessdata.fda.gov/drugsatfda_docs/label/2022/212888s005s006lbl.pdf)>. Accessed February 2023.
3. European Medicines Agency (EMA). Vocabria Product Information <[https://www.ema.europa.eu/en/documents/product-information/vocabria-epar-product-information\\_en.pdf](https://www.ema.europa.eu/en/documents/product-information/vocabria-epar-product-information_en.pdf)>. Accessed February 2023.
4. Hodge, D., Back, D.J., Gibbons, S., Khoo, S.H. & Marzolini, C. Pharmacokinetics and drug–drug interactions of long-acting intramuscular Cabotegravir and Rilpivirine. *Clin. Pharmacokinet.* **60**, 835–853 (2021).
5. European Medicines Agency (EMA). Rekambys Product Information <[https://www.ema.europa.eu/en/documents/product-information/rekambys-epar-product-information\\_en.pdf](https://www.ema.europa.eu/en/documents/product-information/rekambys-epar-product-information_en.pdf)>. Accessed February 2023.
6. Delany-Moretlwe, S. et al. Cabotegravir for the prevention of HIV-1 in women: results from HPTN 084, a phase 3, randomised clinical trial. *Lancet (London, England)* **399**, 1779–1789 (2022).
7. Landovitz, R.J. et al. Cabotegravir for HIV prevention in cisgender men and transgender women. *N. Engl. J. Med.* **385**, 595–608 (2021).
8. U.S. Food and Drug Administration. Apretude product label <[https://www.accessdata.fda.gov/drugsatfda\\_docs/label/2021/215499s000lbl.pdf](https://www.accessdata.fda.gov/drugsatfda_docs/label/2021/215499s000lbl.pdf)>. Accessed March 2023.
9. Han, K. et al. Population pharmacokinetics of cabotegravir following administration of oral tablet and long-acting intramuscular injection in adult HIV-1-infected and uninfected subjects. *Br. J. Clin. Pharmacol.* **88**, 4607–4622 (2022).
10. Yu, Y. et al. A population pharmacokinetic model based on HPTN 077 of long-acting injectable cabotegravir for HIV PreP. *Br. J. Clin. Pharmacol.* **88**, 4623–4632 (2022).
11. Margolis, D.A. et al. Cabotegravir plus rilpivirine, once a day, after induction with cabotegravir plus nucleoside reverse transcriptase inhibitors in antiretroviral-naïve adults with HIV-1 infection (LATTE): a randomised, phase 2b, dose-ranging trial. *Lancet Infect. Dis.* **15**, 1145–1155 (2015).
12. Landovitz, R.J. et al. Tail-phase safety, tolerability, and pharmacokinetics of long-acting injectable cabotegravir in HIV-uninfected adults: a secondary analysis of the HPTN 077 trial. *Lancet HIV* **7**, e472–e481 (2020).
13. Han, K., Baker, M., Margolis, D. et al. Impact of UGT induction by rifampin and Rifabutin on Cabotegravir long-acting pharmacokinetics for HIV pre-exposure prophylaxis (PrEP) using population pharmacokinetic modeling and simulation. *HIVR4P* 27–28 January & 3–4 February (2021).

14. Orkin, C. et al. Initiation of long-acting cabotegravir plus rilpivirine as direct-to-injection or with an oral lead-in in adults with HIV-1 infection: week 124 results of the open-label phase 3 FLAIR study. *Lancet HIV* **8**, e668–e678 (2021).
15. Thoueille, P., et al. Real-world trough concentrations and effectiveness of long-acting cabotegravir and rilpivirine: a multicenter prospective observational study in Switzerland. *Lancet Regional Health Europe* **36**, 100793 (2023). <https://doi.org/10.1016/j.lanepe.2023.100793>
16. Thoueille, P. et al. Guidance for the interpretation of long-acting cabotegravir and rilpivirine concentrations based on real-world Therapeutic Drug Monitoring data and documented failures. *Open Forum Infect. Dis.* **11**, ofae023 (2024). <https://doi.org/10.1093/ofid/ofae023>
17. Scherrer, A.U. et al. Cohort profile update: the Swiss HIV cohort study (SHCS). *Int. J. Epidemiol.* **51**, 33–34j (2022).
18. Courlet, P. et al. Development and validation of a multiplex UHPLC-MS/MS assay with stable isotopic internal standards for the monitoring of the plasma concentrations of the antiretroviral drugs bictegravir, cabotegravir, doravirine, and rilpivirine in people living with HIV. *J Mass Spectrometry* **55**, e4506 (2020).
19. Cabotegravir (Oral) PK Fact Sheet. University of Liverpool. Produced February (2021).
20. Cabotegravir (IM) PK Fact Sheet. University of Liverpool. Produced February (2021).
21. Overton, E.T. et al. Long-acting cabotegravir and rilpivirine dosed every 2 months in adults with HIV-1 infection: 152-week results from ATLAS-2M, a randomized, open-label, phase 3b, noninferiority study. *Clin. Infect. Dis.* **76**, 1646–1654 (2023).
22. Ahn, J.E., Karlsson, M.O., Dunne, A. & Ludden, T.M. Likelihood based approaches to handling data below the quantification limit using NONMEM VI. *J. Pharmacokinet. Pharmacodyn.* **35**, 401–421 (2008).
23. Levey, A.S. et al. A new equation to estimate glomerular filtration rate. *Ann. Intern. Med.* **150**, 604–612 (2009).
24. Child, C.G. & Turcotte, J.G. Surgery and portal hypertension. *Major Probl. Clin. Surg.* **1**, 1–85 (1964).
25. Bettone, S., Berton, M., Stader, F., Battegay, M. & Marzolini, C. Management of drug-drug interactions between long-acting cabotegravir and rilpivirine and comedications with inducing properties: a modelling study. *Clin. Infect. Dis.* **76**, 1225–1236 (2022).
26. Lindbom, L., Pihlgren, P. & Jonsson, E.N. PsN-toolkit – a collection of computer intensive statistical methods for non-linear mixed effect modeling using NONMEM. *Comput. Methods Prog. Biomed.* **79**, 241–257 (2005).
27. Bergstrand, M., Hooker, A.C., Wallin, J.E. & Karlsson, M.O. Prediction-corrected visual predictive checks for diagnosing nonlinear mixed-effects models. *AAPS J.* **13**, 143–151 (2011).
28. Jonsson, E.N. & Karlsson, M.O. Xpose – an S-PLUS based population pharmacokinetic/pharmacodynamic model building aid for NONMEM. *Comput. Methods Prog. Biomed.* **58**, 51–64 (1999).
29. Sheiner, L.B. & Beal, S.L. Some suggestions for measuring predictive performance. *J. Pharmacokinet. Biopharm.* **9**, 503–512 (1981).
30. Savic, R.M. & Karlsson, M.O. Importance of shrinkage in empirical bayes estimates for diagnostics: problems and solutions. *AAPS J.* **11**, 558–569 (2009).
31. Jucker, B.M. et al. Multiparametric magnetic resonance imaging to characterize cabotegravir long-acting formulation depot kinetics in healthy adult volunteers. *Br. J. Clin. Pharmacol.* **88**, 1655–1666 (2021).
32. Glenmark, B., Nilsson, M., Gao, H., Gustafsson, J.-Å., Dahlman-Wright, K. & Westerblad, H. Difference in skeletal muscle function in males vs. females: role of estrogen receptor- $\beta$ . *Am J Physiol-Endocrinol Metabol* **287**, E1125–E1131 (2004).
33. Cutrell, A.G. et al. Exploring predictors of HIV-1 virologic failure to long-acting cabotegravir and rilpivirine: a multivariable analysis. *AIDS* **35**, 1333–1342 (2021).
34. Orkin, C. et al. Expanded multivariable models to assist patient selection for long-acting Cabotegravir+Rilpivirine treatment: clinical utility of a combination of patient, drug concentration, and viral factors associated with Virologic failure. *Clin. Infect. Dis.* **77**, 1423–1431 (2023).
35. Elliot, E. et al. Efficacy, safety, and pharmacokinetics by BMI category in phase 3/3b cabotegravir+rilpivirine long-acting trials. *J. Infect. Dis.* (2023). <https://doi.org/10.1093/infdis/jiad580>
36. Bettone, S., Berton, M., Stader, F., Battegay, M. & Marzolini, C. Effect of obesity on the exposure of long-acting cabotegravir and rilpivirine: a modelling study. *Clin. Infect. Dis.* (2024). <https://doi.org/10.1093/cid/ciae060>
37. Marzinke, M.A. et al. Cabotegravir pharmacology in the background of delayed injections in HPTN 084. Oral Abstract Session-08. Conference on Retroviruses and Opportunistic Infections (CROI), February 19–22- Seattle, WA, USA (2023).
38. Hazra, A., Landovitz, R.J., Marzinke, M.A., Quinby, C. & Creticos, C. Breakthrough HIV-1 infection in setting of cabotegravir for HIV pre-exposure prophylaxis. *AIDS* **37**, 1711–1714 (2023).
39. Han, K. et al. Pharmacokinetics and tolerability of cabotegravir and rilpivirine long-acting intramuscular injections to the vastus lateralis (lateral thigh) muscles of healthy adult participants. *Antimicrob. Agents Chemother.* **68**, e0078123 (2024). <https://doi.org/10.1128/aac.00781-23>
40. Felizarta, F. et al. Thigh injections of Cabotegravir + Rilpivirine in virally suppressed adults with HIV-1. Conference on Retroviruses and Opportunistic Infections (CROI), February 19–22-Seattle, WA, USA (2023).
41. Ullah Nayan, M. et al. Advances in long-acting slow effective release antiretroviral therapies for treatment and prevention of HIV infection. *Adv. Drug Deliv. Rev.* **115009**, 115009 (2023).
42. Young, I.C. et al. Dose-ranging plasma and genital tissue pharmacokinetics and biodegradation of ultra-long-acting Cabotegravir in situ forming implant. *Pharmaceutics* **15**, 1487 (2023). <https://doi.org/10.3390/pharmaceutics15051487>